Electronic Supplementary Material (ESI) for Journal of Materials Chemistry A.

Electronic Supplementary Information

Boosting Transport Kinetics of Free-Standing SnS_2@Carbon Nanofibers by Electronic Structure Modulation for Advanced Lithium Storage

Hui Jiang,[a, 1] Yang Gan,[a, 1] Jie Liu,[a] Xunlu Wang,[a] Ruguang Ma,[c] Jianjun Liu*[a] and Jiacheng Wang*[a, b]

[a.] State Key Laboratory of High-Performance Ceramics and Superfine Microstructure, Shanghai Institute of Ceramics, Chinese Academy of Sciences, Shanghai 200050, China.

[b.] Center of Materials Science and Optoelectronics Engineering, University of Chinese Academy of Sciences, Beijing 100049, China

[c.] School of Materials Science and Engineering, Suzhou University of Science and Technology, 99 Xuefu Road Suzhou, 215011, China.

[1] These authors contributed equally to this work.

Email: jliu@mail.sic.ac.cn; jiacheng.wang@mail.sic.ac.cn

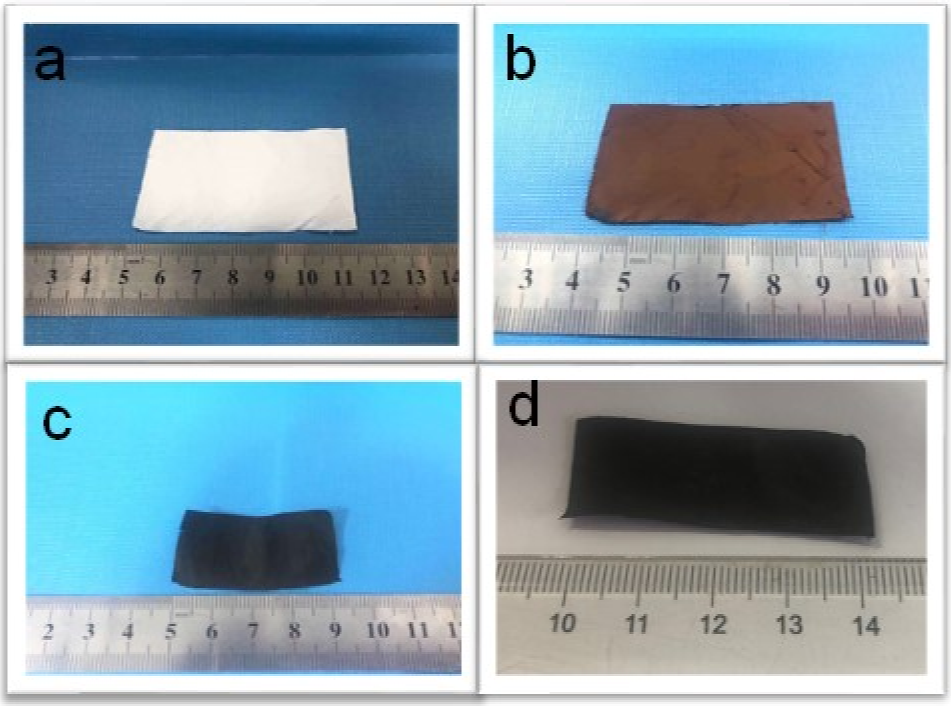

Fig S1. Digital photos of a) Sn, Mg-containing polymer membrane. The membrane was calcinated at 250 ^{o}C in air b), sintered at 700 ^{o}C in Ar c). d) The final free-standing electrodes after a sulfidation process.

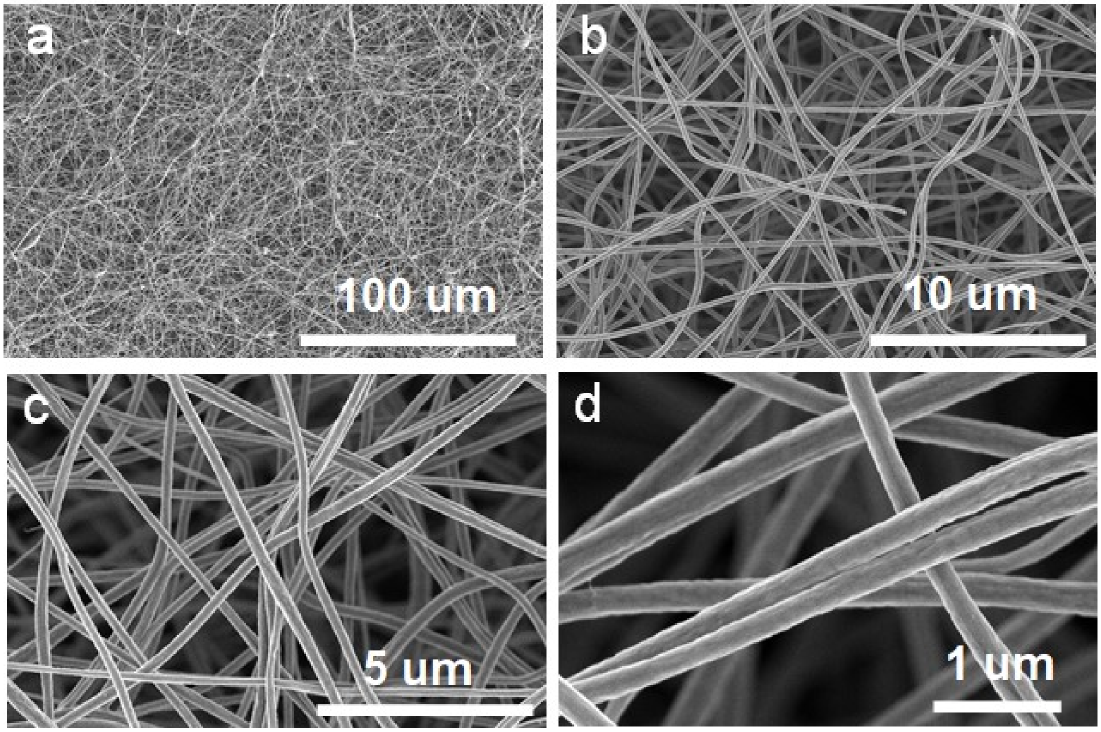

Fig S2. The SEM images of Sn/CNFs.

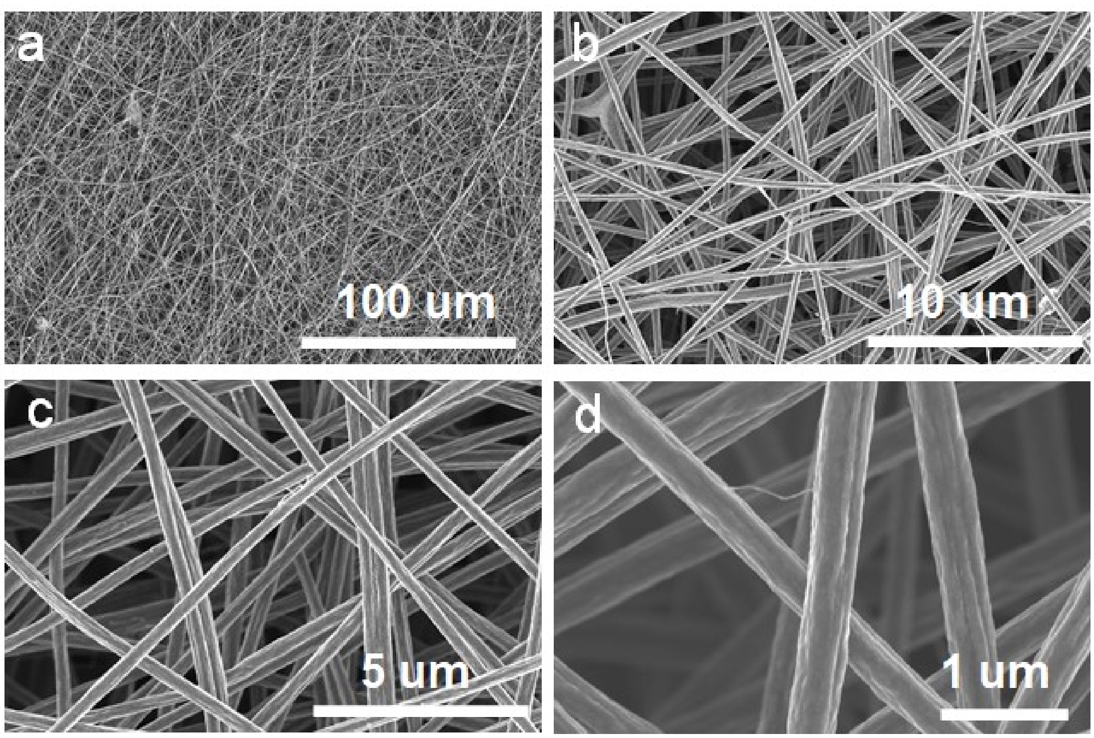

Fig S3. SEM images of Mg-Sn/CNFs.

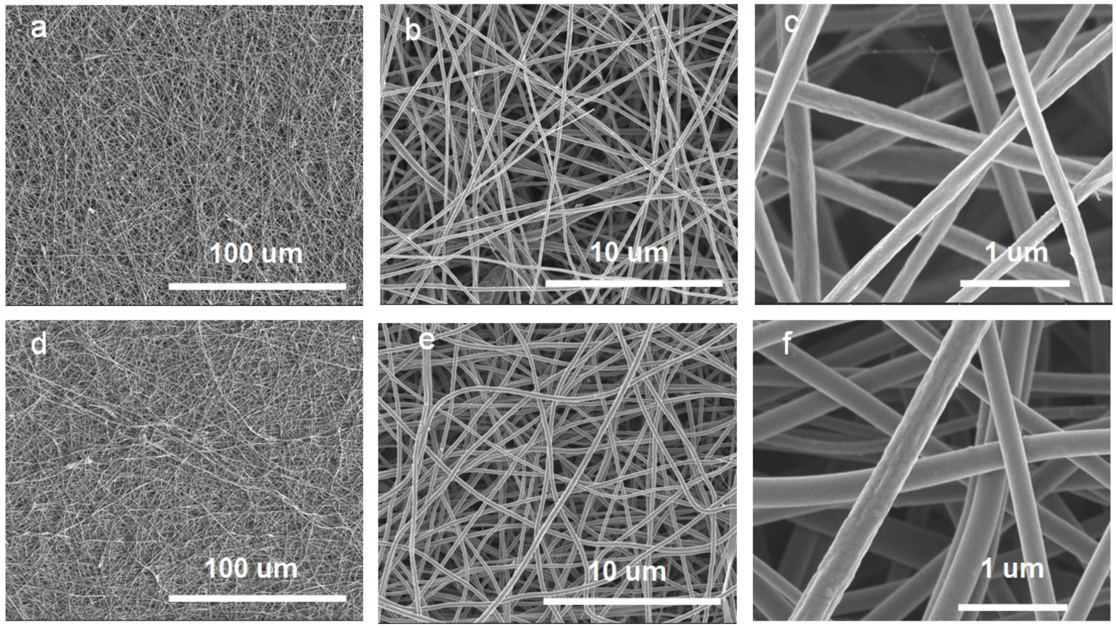

Fig S4. SEM images of SnS_2/CNFs (a-c) and Mg-SnS_2/CNFs (d-f).

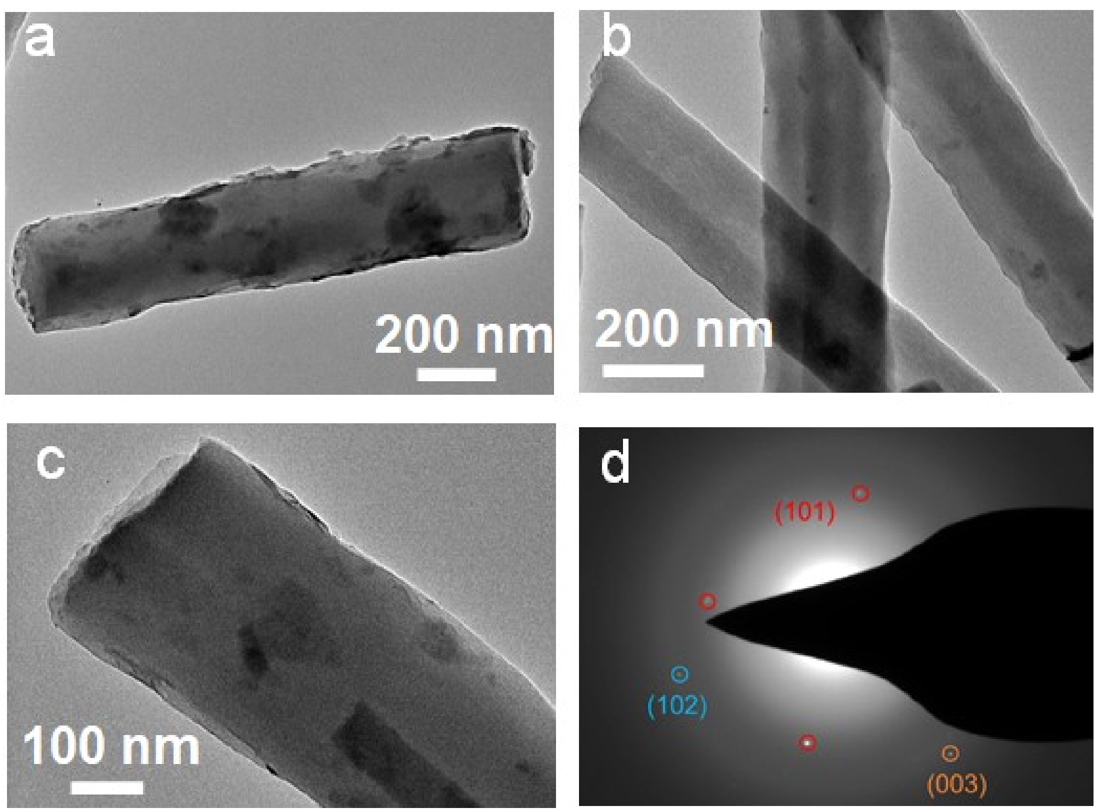

Fig S5. TEM images of SnS_2/CNFs (a-c); Corresponding SAED images of SnS_2/CNFs (d).

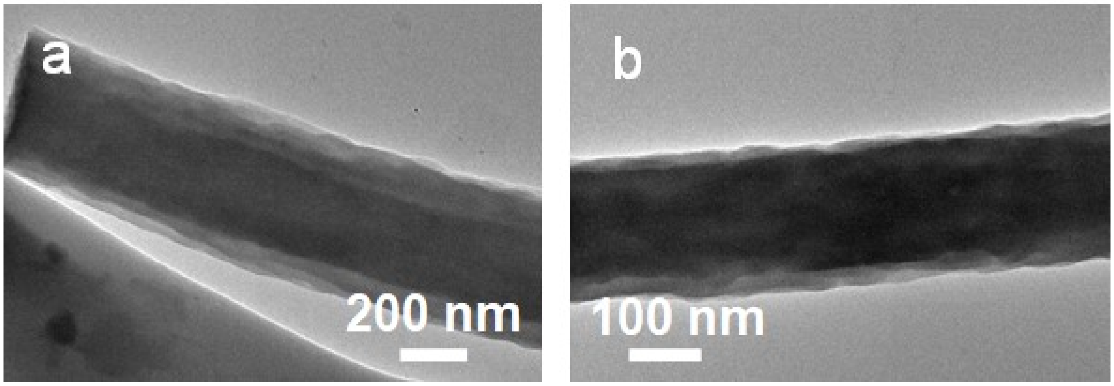

Fig S6. TEM images of Mg-SnS_2/CNFs (a-b).

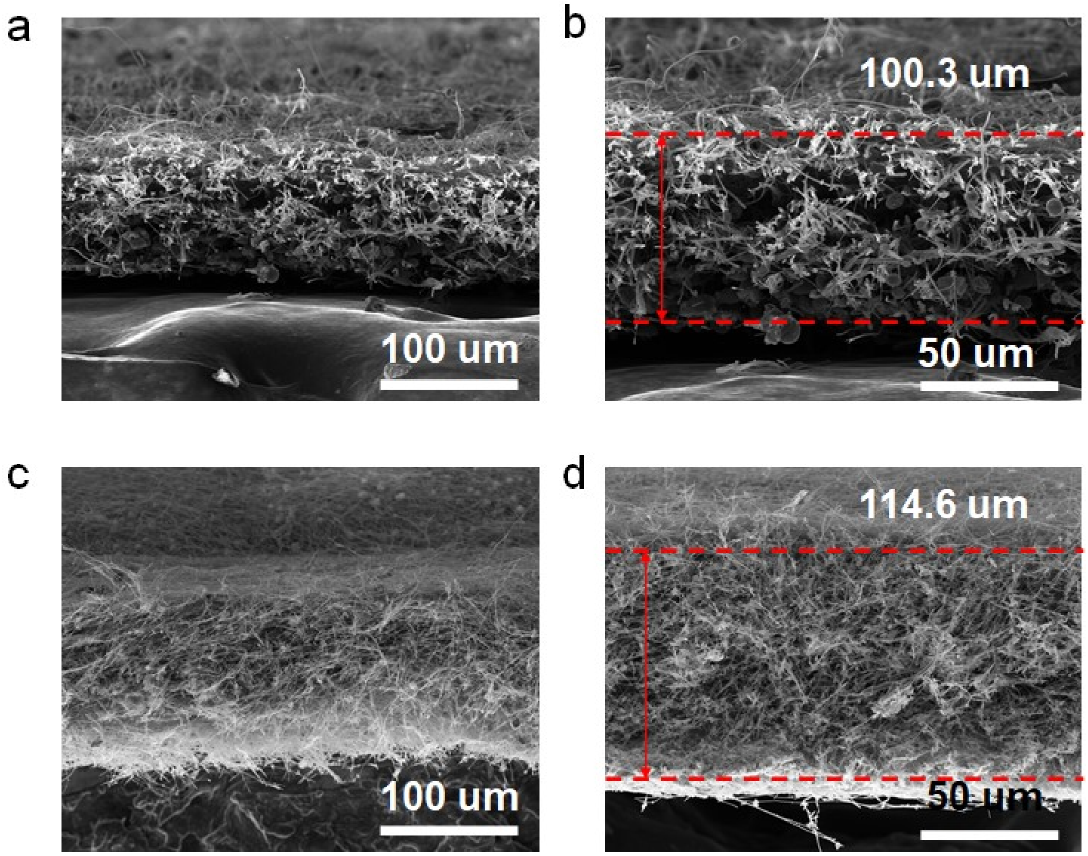

Fig S7. Cross-sectional SEM images of the (a-b) SnS_2/CNFs and (c-d) Mg-SnS_2/CNFs electrodes before cycling.

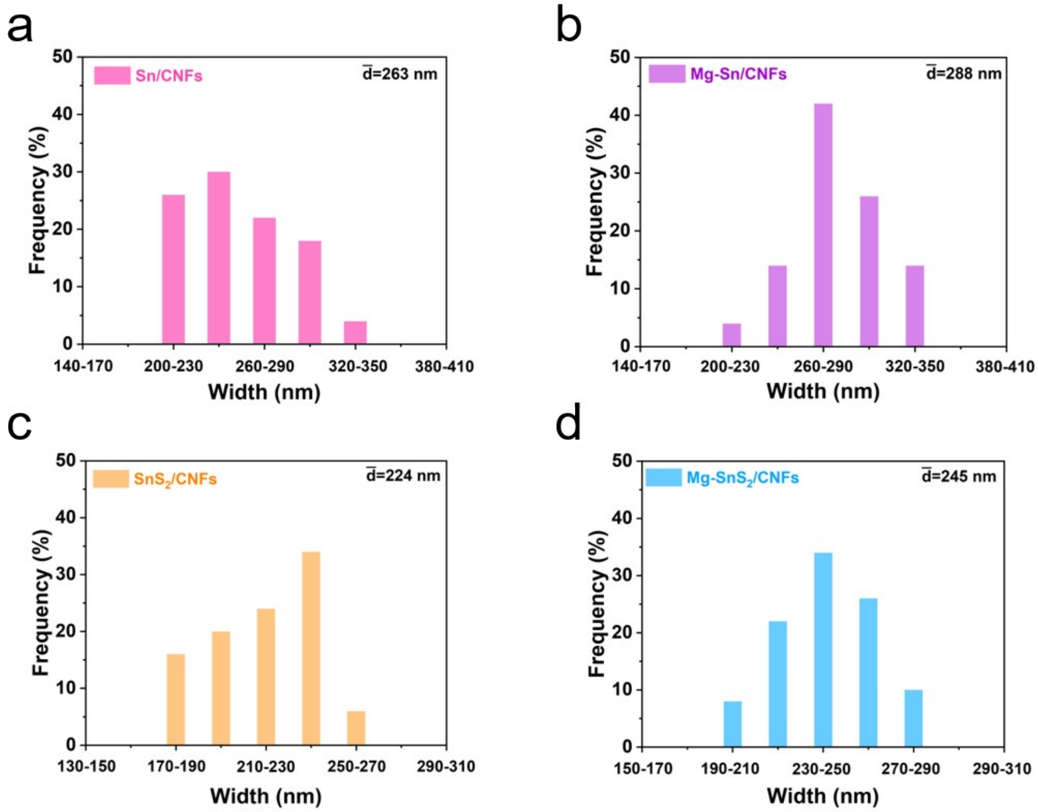

Fig S8. Fiber width distributions of Sn/CNFs (a), Mg-Sn/CNFs (b), SnS_2/CNFs (c), and Mg-SnS_2/CNFs (d).

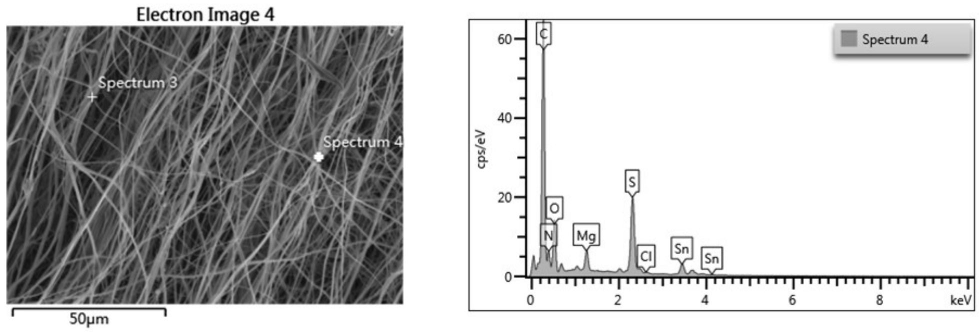

Element	Wt%	Wt% Sigma	Atomic %
C	63.41	0.72	80.59
N	1.67	1.04	1.82
O	9.27	0.17	8.85
Mg	1.86	0.05	1.17
S	12.73	0.18	6.06
Cl	0.29	0.05	0.12
Sn	10.76	0.26	1.38
Total:	100.00		100.00

Fig S9. a) SEM image, b) EDX spectrum of Mg-SnS_2/CNFs and c) the corresponding elemental content.

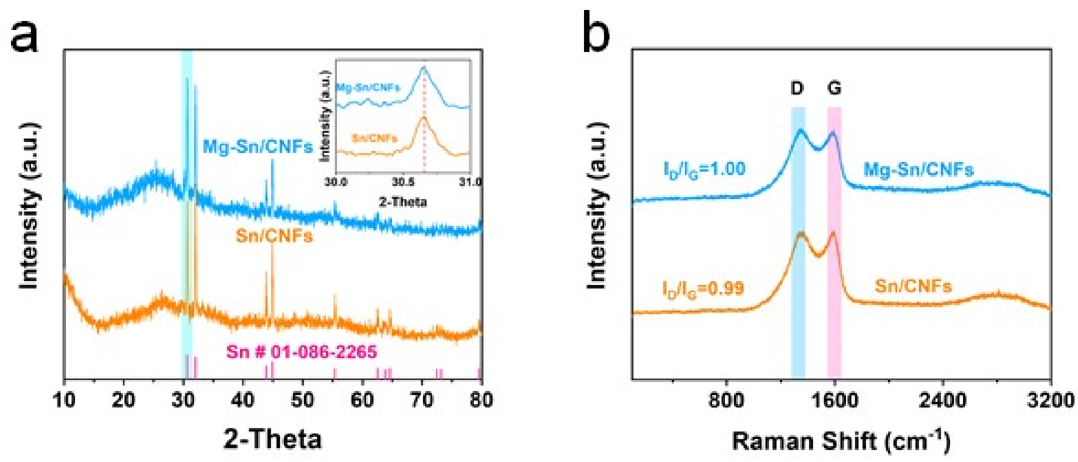

Fig S10. XRD patterns of (a) Sn/CNFs and Mg-Sn/CNFs. (b) Raman spectra of Sn/CNFs and Mg-Sn/CNFs.

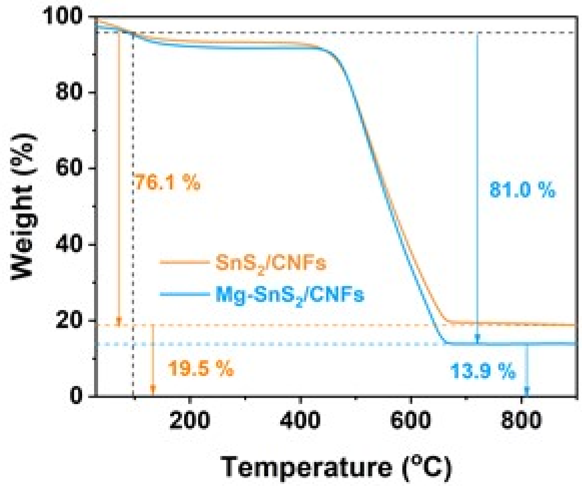

Fig S11. TGA curves of SnS_2/CNFs and Mg-SnS_2/CNFs.

$$n = \frac{n_2}{n_1 + n_2} \times \frac{M_{SnS_2}}{M_{SnO_2}} = \frac{19.5\%}{19.5\% + 76.1\%} * \frac{182.9}{150.4} = 24.8\%$$

Where n_1 represents the weight of percentage of carbon nanofibers, n_2 represents the mass of final production, M_{SnS_2} represents the mole mass of SnS_2, and M_{SnO_2} represents the mole mass of SnO_2.

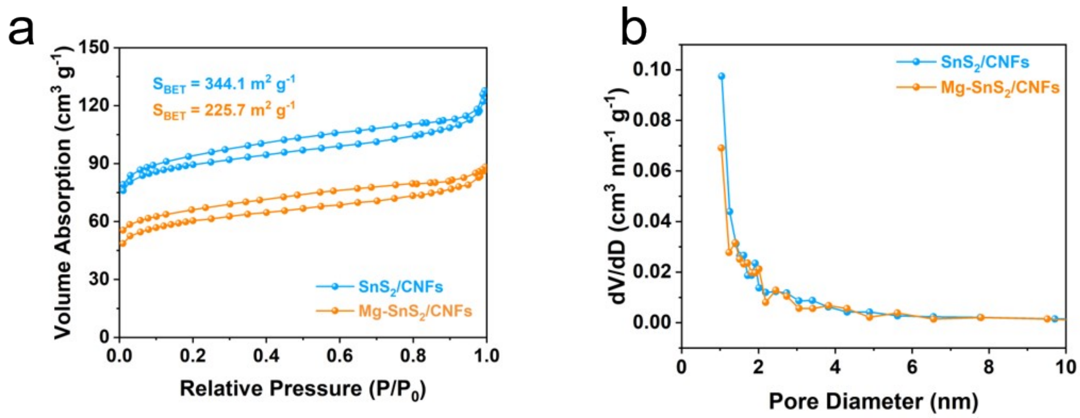

Fig S12. (a) The N_2 adsorption-desorption analysis of SnS_2/CNFs and Mg-SnS_2/CNFs. (b) The pore size distribution of SnS_2/CNFs and Mg-SnS_2/CNFs.

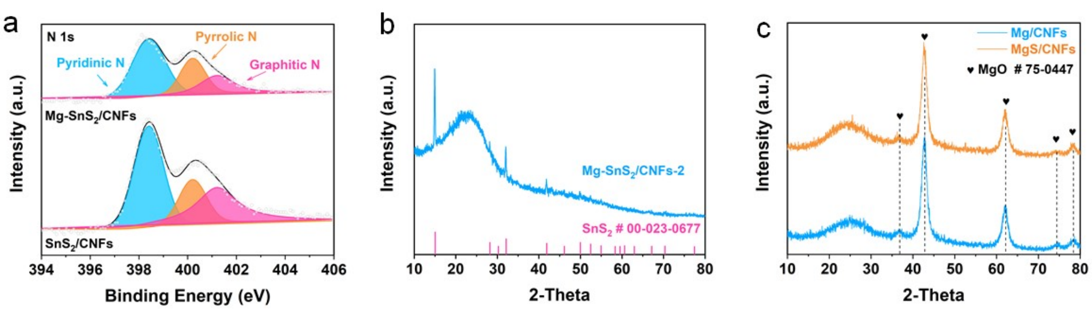

Fig S13. (a) XPS spectra of the SnS_2/CNFs and Mg-SnS_2/CNFs electrode for N 1s. (b) XRD patterns of Mg-SnS_2/CNFs-2. (c) XRD patterns of Mg/CNFs and Mg-S/CNFs.

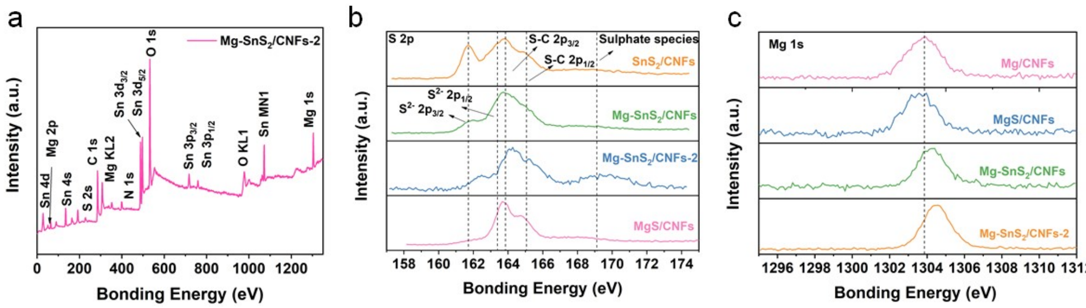

Fig S14. (a) XPS survey spectrum of the Mg-SnS_2/CNFs-2. Corresponding high-resolution spectrum of (b) S 2p and (c) Mg 1s for Mg/CNFs, Mg-S/CNFs, Mg-SnS_2/CNFs, Mg-SnS_2/CNFs-2, and SnS_2/CNFs.

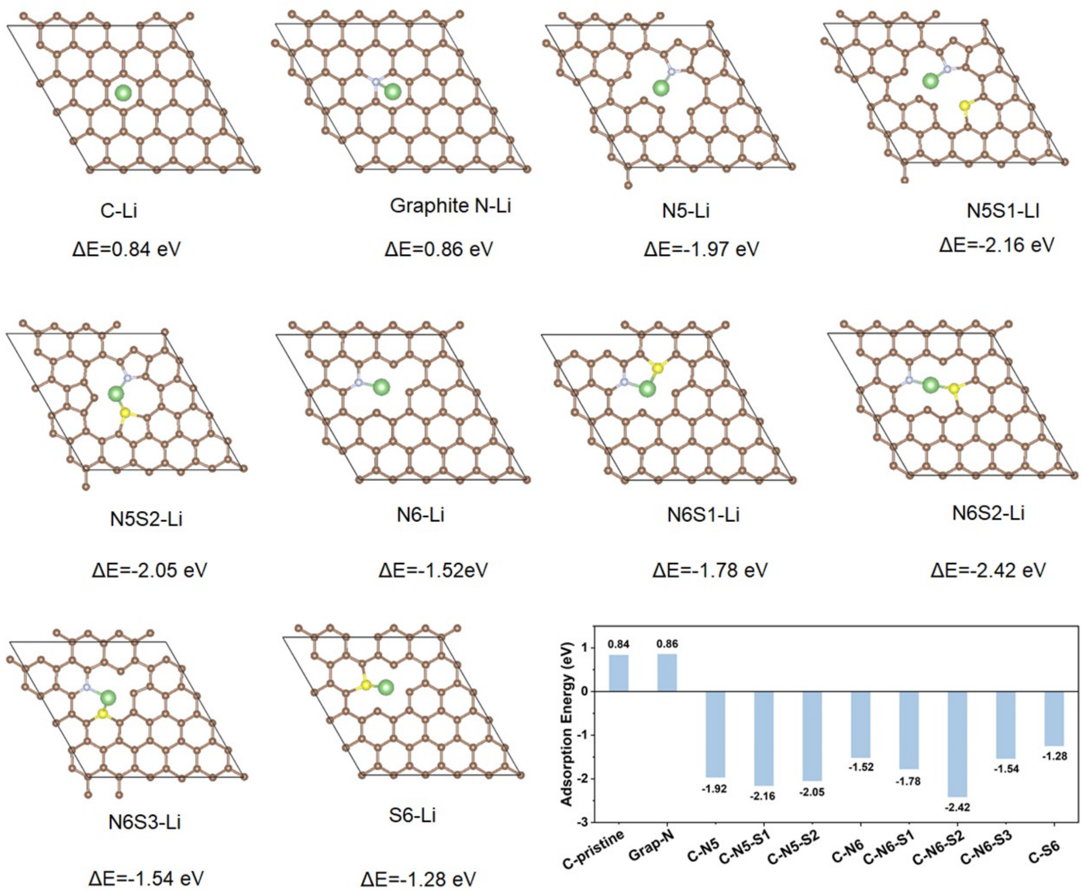

Fig S15. Theoretical results of Li adsorption on various sites (brown-carbon, yellow-sulfur, and green-lithium) and a survey of the calculated values of the adsorption energy.

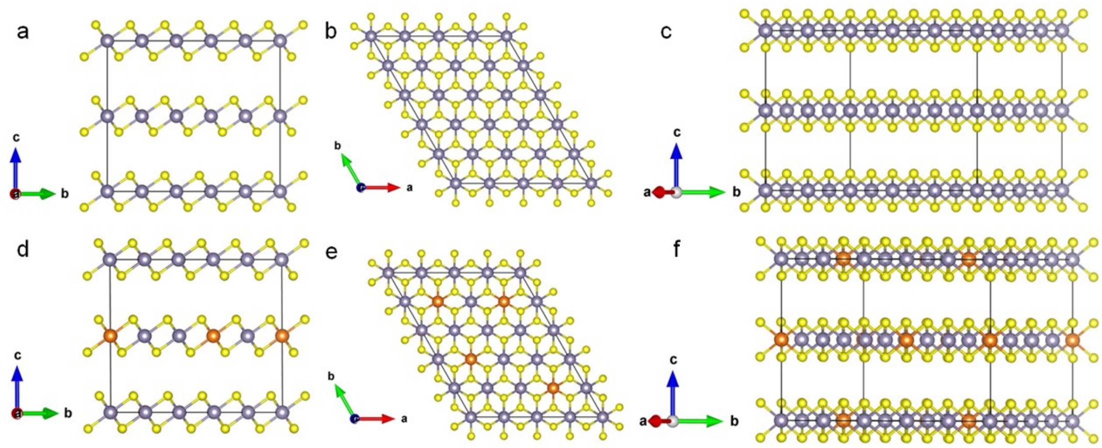

Fig S16. The detailed structure of SnS_2 (a-c) and Mg-SnS_2 (d-f) at different perspectives.

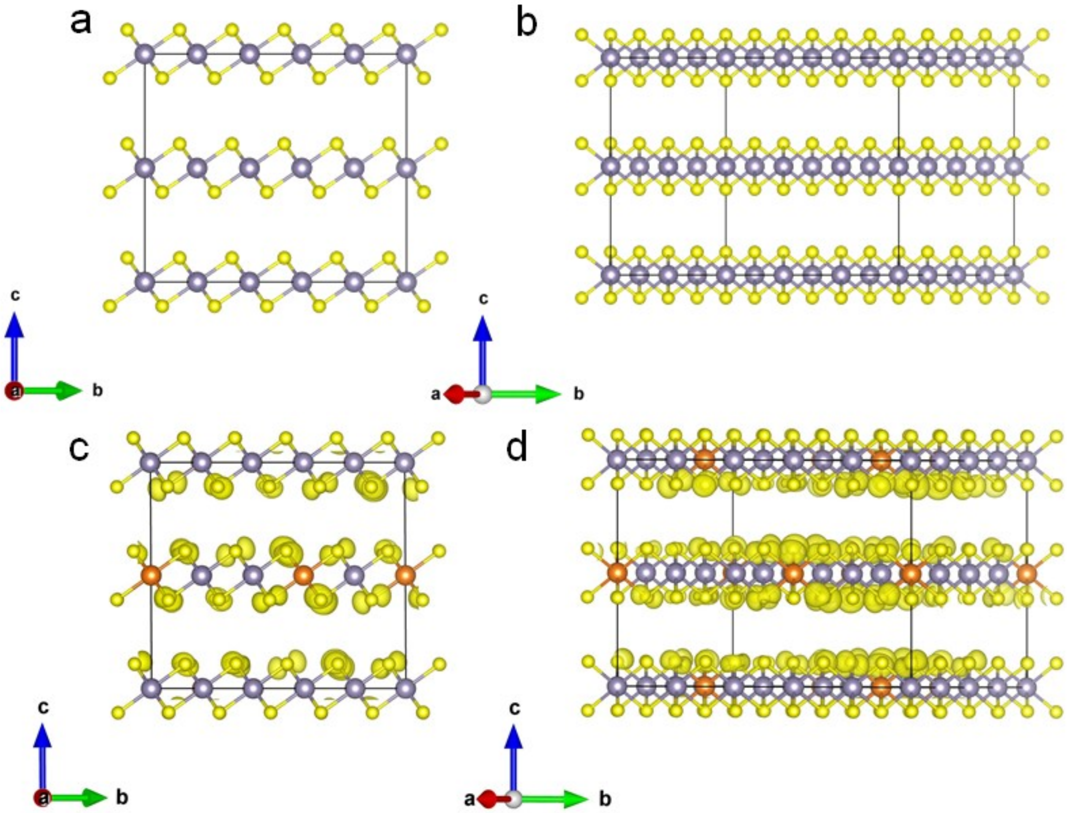

Fig S17. Calculated spin density distribution of pure (a-b) and Mg-doped (c-d) SnS_2 (isosurface level = 2.696×10^{-3} e/Å^3) at different perspectives.

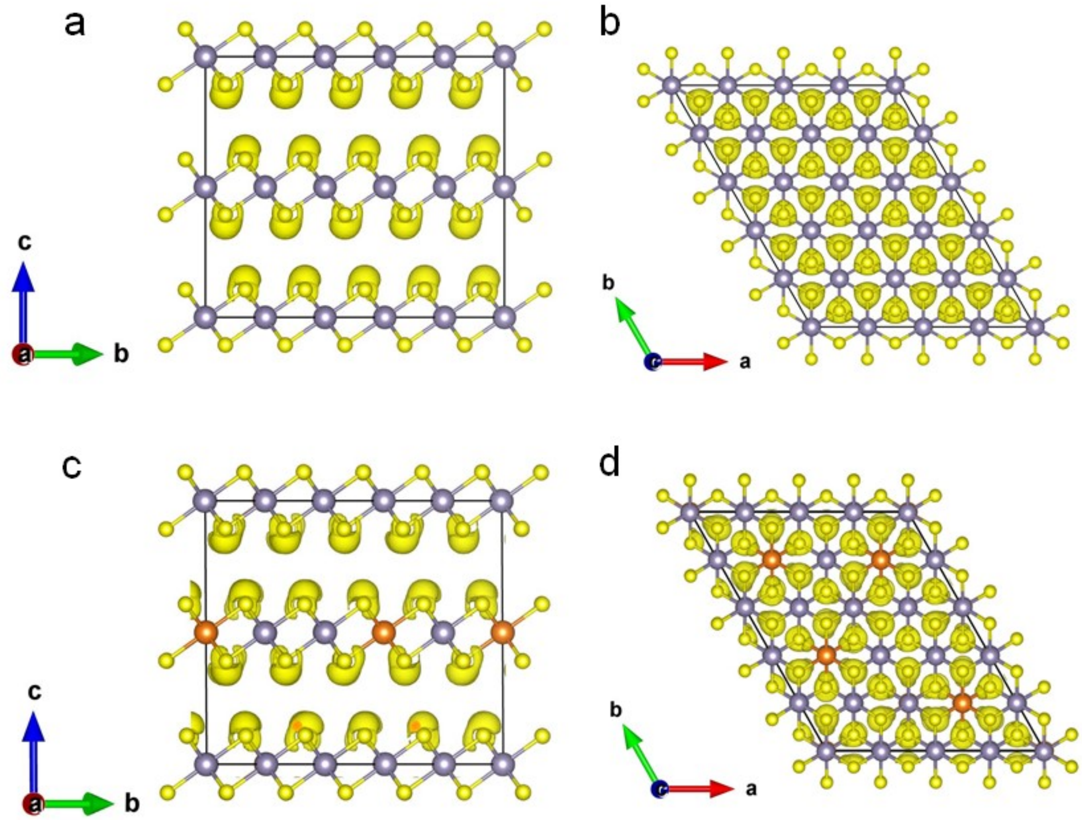

Fig S18. Electron Localization Function profile of pure (a-b) and Mg-doped (c-d) SnS_2 on (100) at different perspectives.

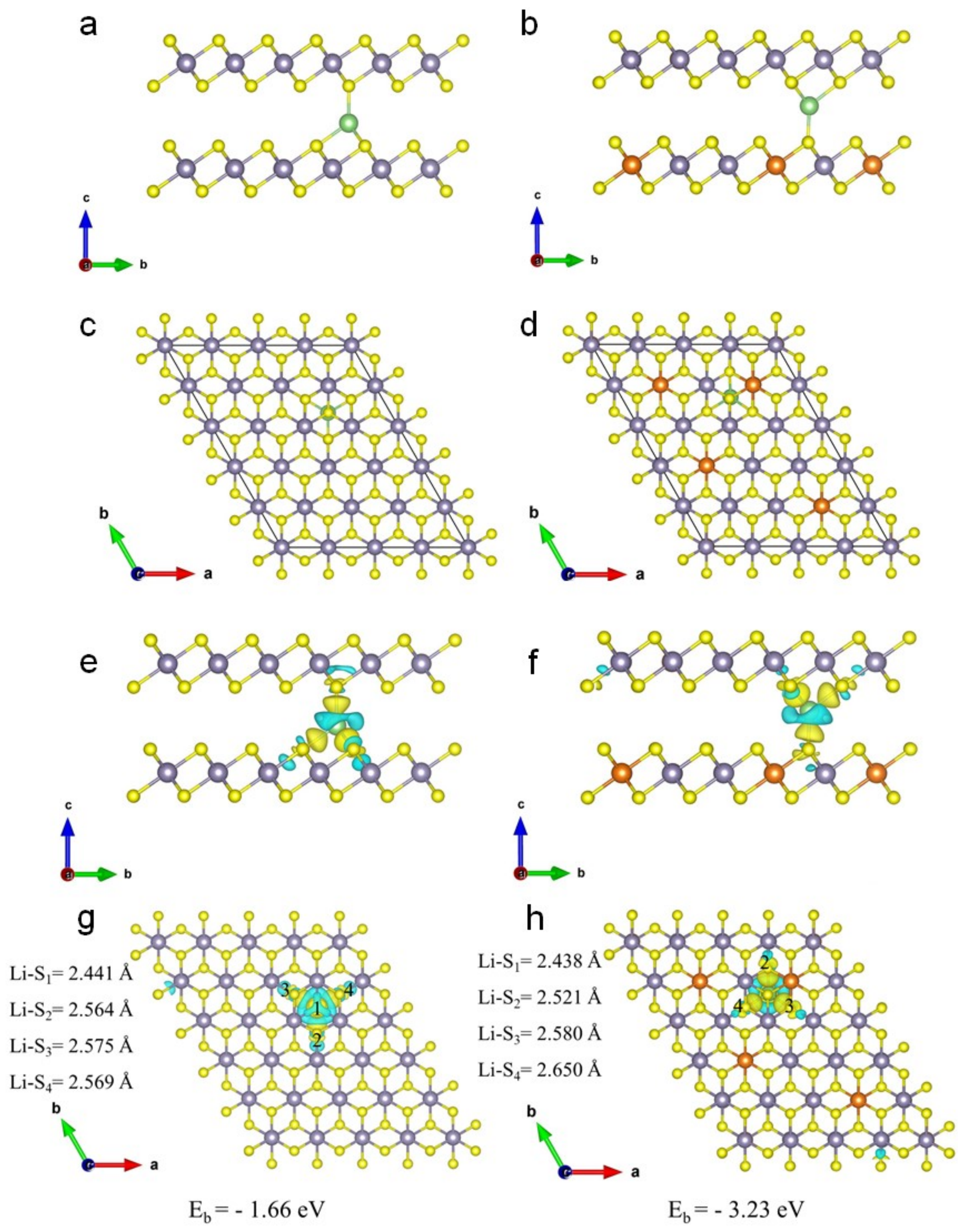

Fig S19. The binding stability of Li intercalated into interlayer for SnS_2 (a, c) and Mg-SnS_2 (b, d). The charge density differences after Li intercalated in to interlayer for SnS_2 (e, g) and Mg-SnS_2 (f, h).

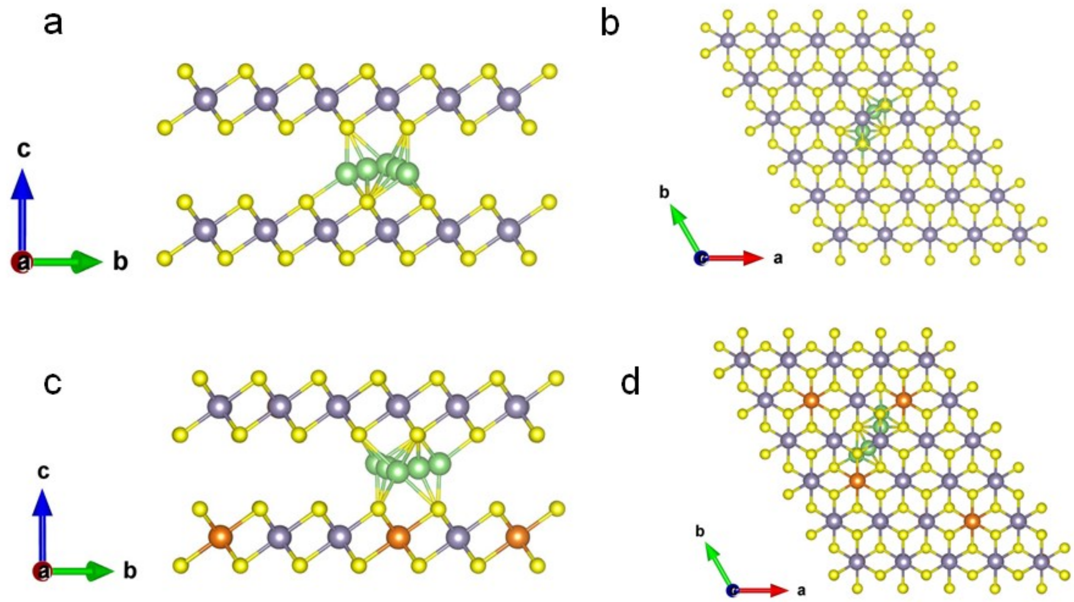

Fig S20. The Schematic representations of corresponding diffusion pathways for (a) SnS_2 and (d) Mg-SnS_2.

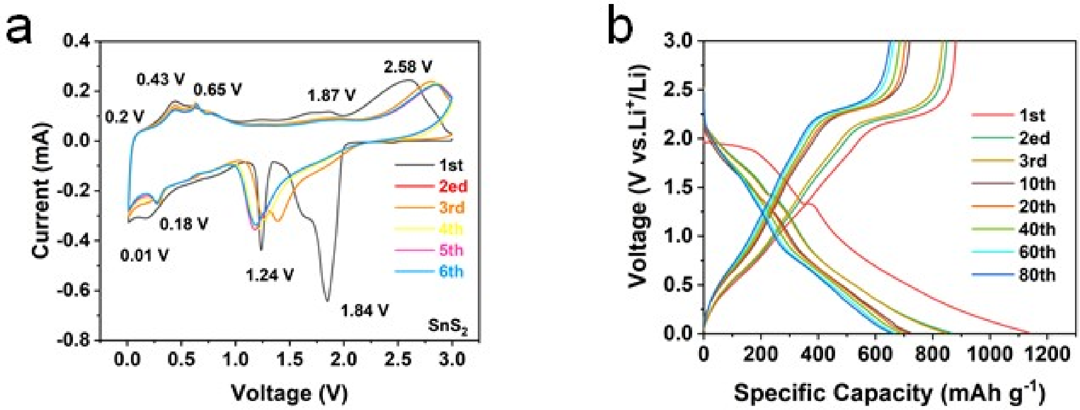

Fig S21. (a) CV curves of SnS_2/CNFs at 0.1 mV s^{-1}. (b) Charge-discharge profiles of SnS_2/CNFs electrode at 0.3 A g^{-1} and activated at 0.1 A g^{-1} for three cycles.

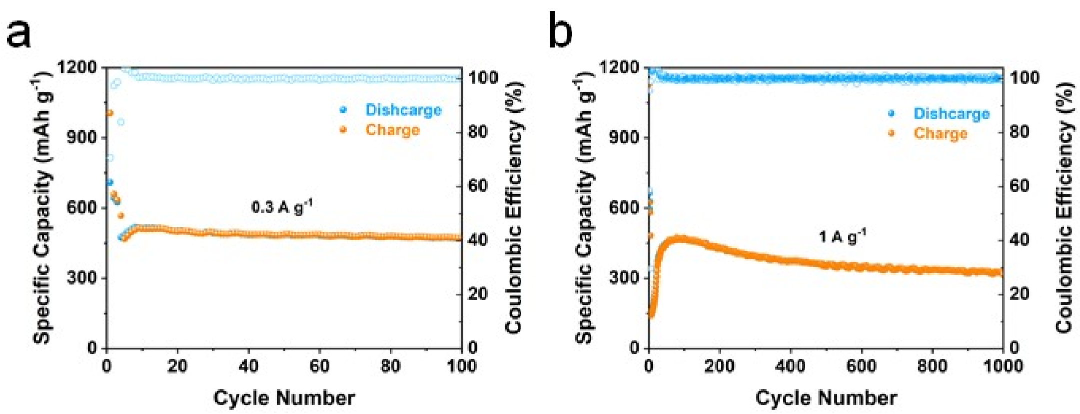

Fig S22. Cycling performance for Mg-SnS_2/CNFs-2 at (a) 0.3 A g^{-1} and (b) 1 A g^{-1} (the electrode was activated at 0.1 A g^{-1} for three cycles).

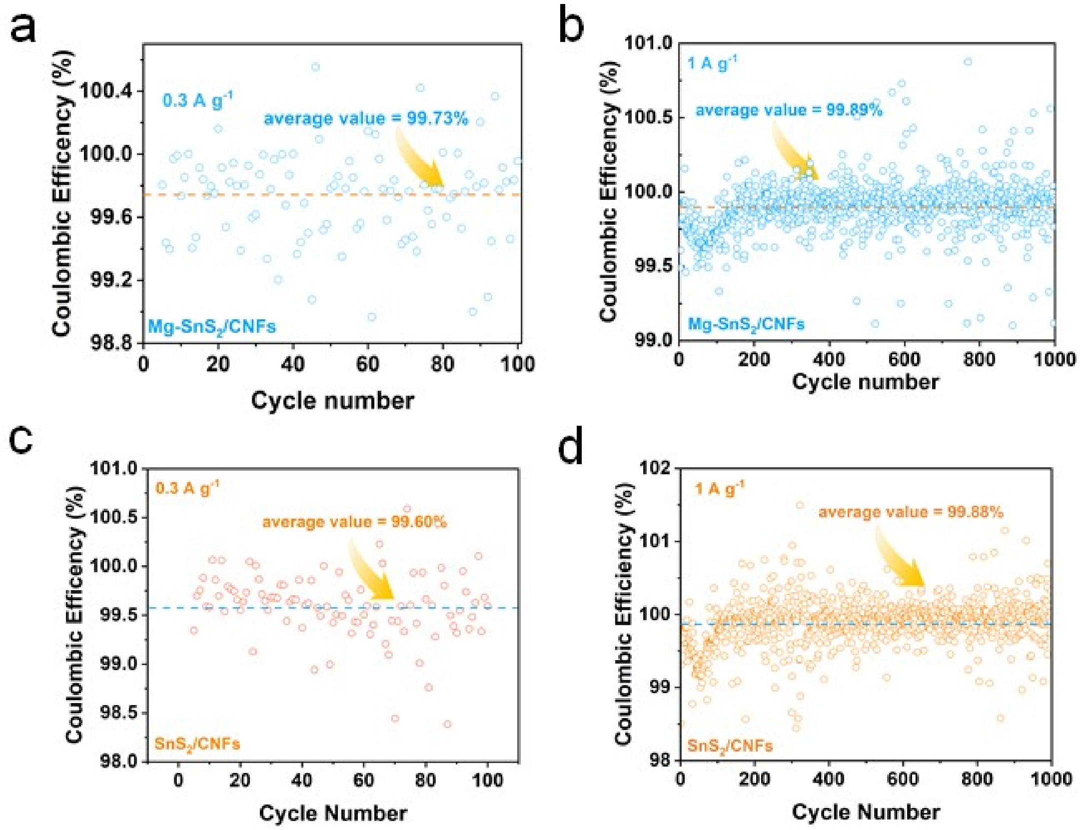

Fig S23. Coulombic efficiencies during cycling for (a, b) Mg-SnS_2/CNFs and (c, d) SnS_2/CNFs at 0.3 A g^{-1} and 1 A g^{-1}.

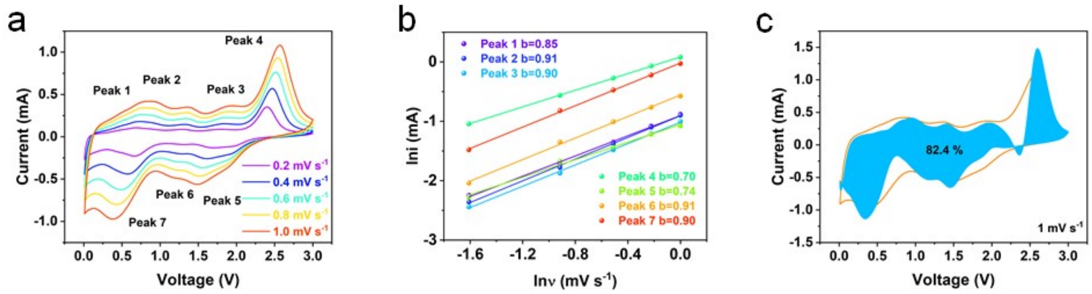

Fig S24. (a) Various scan rates of the SnS_2/CNFs electrode. (b) Plots for b-value determination. (c) Sketch of the capacitive behavior of the SnS_2/CNFs electrode at 1 mV s^{-1}.

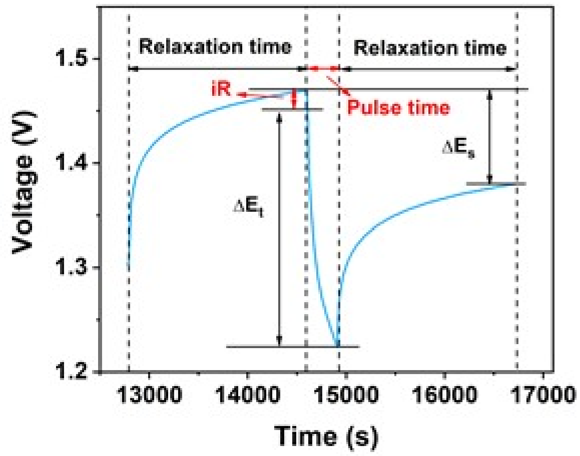

Fig S25. A single GITT curve.

The lithium diffusion coefficient was measured by using Galvanostatic intermittent titration technique (GITT) and calculated based on equation S1 as follows.

$$D = \frac{4L^2}{\pi\tau}(\frac{\Delta E_S}{\Delta E_t})^2$$

Where t is the duration of the current pluse (s), τ is the relaxation time (s), and ΔE_s is the steady-state potential (V) by the current pluse. ΔE_t is the potential change (V) during the constant current pluse after eliminating the iR drop (Figure S7). L is lithium-ion diffusion length (cm); for compact electrode, it is equal to thickness of electrode.

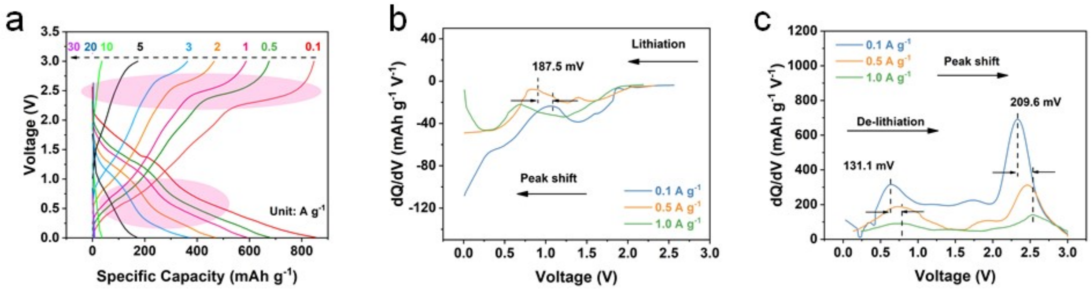

Fig S26. (a) Charge-discharge curves, and dQ/dV profiles of the (b) lithiation and (c) de-lithiation processes of the SnS_2/CNFs electrode at 0.1, 0.5, and 1 A g^{-1}.

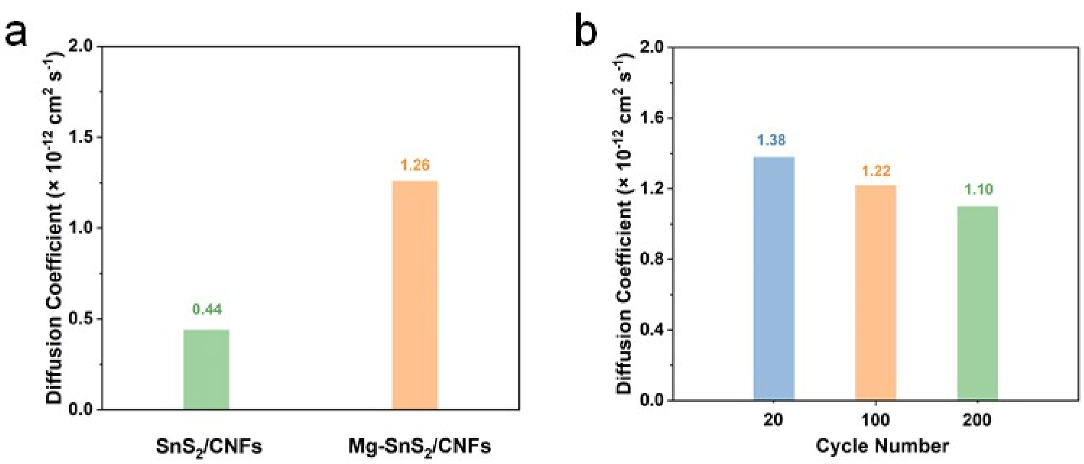

Fig S27. (a) Diffusion coefficient of SnS_2/CNFs and Mg-SnS_2/CNFs after 150 cycles. (b)

Diffusion coefficient of Mg-SnS_2/CNFs after 20, 100, and 200 cycles.

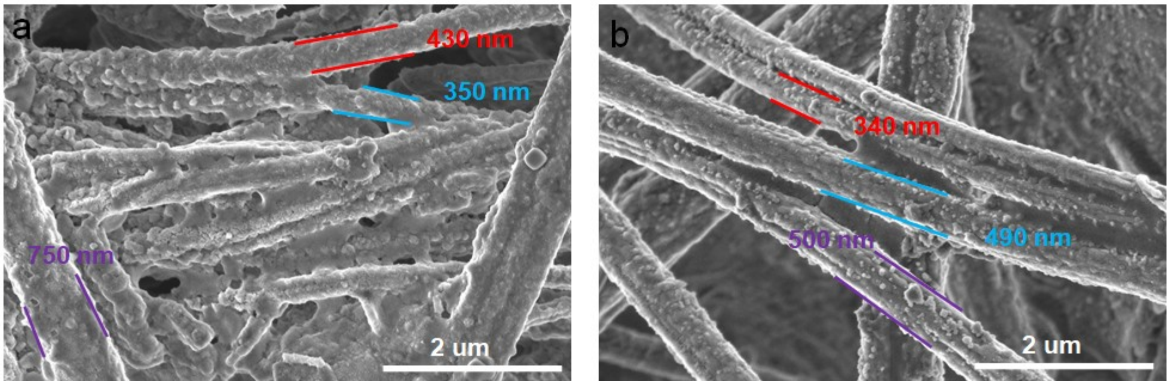

Fig S28. SEM images of (a) SnS_2/CNFs and (b) Mg-SnS_2/CNFs after 100 cycles.

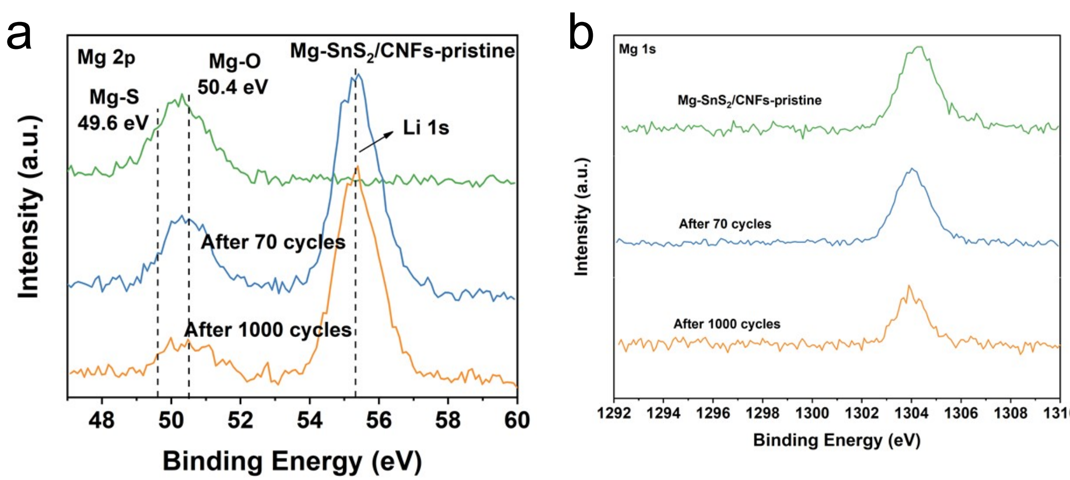

Fig S29. High-resolution spectrum of (a) Mg 2p and (b) Mg 1s.

Table S1. Elemental content of Mg-SnS_2/CNFs and SnS_2/CNFs by ICP.

	Sn atomic %)	Mg (atomic %)
Mg-SnS_2/CNFs	0.56	0.44

Table S2. Elemental content of Mg-SnS_2/CNFs and SnS_2/CNFs by XPS.

		C	N	O	S	Sn	Mg
Mg-SnS_2/CNFs	wt. %	51.01	5.99	15.84	14.53	11.45	1.19
	at. %	67.81	6.83	15.81	7.24	1.54	0.78
SnS_2/CNFs	wt. %	42.93	9.13	12.71	14.48	20.77	0
	at. %	63.3	11.54	14.07	8.00	3.10	0

Table S3. The summary of the lithium storage performance of free-standing anodes.

Materials	ICE [%]	Capacity [mAh g^{-1}] (Cycle, Current Density (A g^{-1}))	Rate Capacity [mAh g^{-1}] (Current Density [A g^{-1}])	Ref.
This Work	**77.4**	**878.7 (100, 0.3)/ 792.5 (100, 1)**	**354.7 (20)/ 207.1 (30)**	**-**
SnS/CBC	61	872 (100, 0.1)	527 (2)	[1]
ALD-SnN_x	58	540 (70, 0.1)	342.7 (1.5)	[2]
LMNP@CS	-	552 (1000, 1)	499 (2)	[3]
SnSb-CNTs@NCNFs	75.0	815 (100, 0.1)	370 (5)	[4]
SnS/C-CP	42	696.2 (200, 0.5)	423.2 (2)	[5]
SnS/C	70.3	548 (500, 0.2)	206 (4)	[6]
Mo-doped SnO_2	40.8	670.5 (700, 0.5)	380 (2)	[7]
10N-SnO_2@CNF	62	909 (100, 0.1)	535 (5)	[8]
V_2O_3/MCCNFs-3	65.5	881.1 (240, 0.1)	456.8 (5)	[9]
FNiO/GP	67	359 (600, 1)	340 (2)	[10]
BP@NC	57.6	1085.1 (200, 0.1)	446.8 (2)	[11]
CC-Co-Ti-350	74	1070 (600, 0.2)	400 (1.6)	[12]
Fe_xO_y/NC-MOG	63.3	879.7 (50, 0.1)	629.3 (1)	[13]
P@PMCNFs/ CNTs	-	802.3 (500, 1)	601 (3)	[14]
TiO_2@MCNFs	74.2	617 (100, 0.1)	210 (1)	[15]

Table S4. The fitting resistance results for SnS_2/CNFs and Mg-SnS_2/CNFs after 150 cycles.

	R_s [Ω]	R_{SEI} [Ω]	R_{ct} [Ω]	CPE_{SEI} [μMho]	CPE_{ct} [μMho]
SnS_2/CNFs	5.56	117	57.9	81.3	2610
Mg- SnS_2/CNFs	6.34	31.8	38.4	270	44800

Table S5. The fitting resistance results for SnS_2/CNFs and Mg-SnS_2/CNFs at different cycles.

	R_s [Ω]	R_{SEI} [Ω]	R_{ct} [Ω]	CPE_{SEI} [μMho]	CPE_{ct} [μMho]
20 cycles	4.08	96.8	58.7	10.0	4710
100 cycles	5.00	54.1	51.1	24.8	2180
200 cycles	5.42	21.1	25.4	389	38500

Table S6. The fitting resistance results for SnS_2/CNFs and Mg-SnS_2/CNFs at different temperatures.

	R_s [Ω]	R_{SEI} [Ω]	R_{ct} [Ω]	CPE_{SEI} [μMho]	CPE_{ct} [μMho]
SnS_2/CNFs-25	5.00	73.9	142	24.7	1230
SnS_2/CNFs-45	4.19	21.6	110	27.4	1260
SnS_2/CNFs-65	3.32	3.43	82.1	4.57	1870
Mg- SnS_2/CNFs-25	4.83	80	44.7	29.9	860
Mg- SnS_2/CNFs-45	4.02	19.8	33.4	40.8	1460
Mg- SnS_2/CNFs-65	3.77	9.45	28.2	36.6	1480

Table S7. The elemental content of C, O, S, Sn and Mg before and after cycling.

	Cycles	C	O	S	Sn	Mg
Mg-SnS_2/CNFs (at. %)	0	72.78	16.97	7.77	1.65	0.84
	70	45.59	49.07	2.51	2.09	0.75
	1000	45.85	50.00	3.25	0.68	0.21
SnS_2/CNFs (at. %)	0	71.55	15.90	9.04	3.50	0
	70	44.23	49.66	3.96	2.15	0
	1000	41.18	50.28	5.69	2.29	0

References

1 F. Yuan, Y. Huang, J. Qian, M. M. Rahman, P. M. Ajayan and D. Sun, *Carbohydr. Polym.*, 2021, **255**, 117400.

2 M. Z. Ansari, D. K. Nandi, P. Janicek, S. A. Ansari, R. Ramesh, T. Cheon, B. Shong and S.-H. Kim, *ACS Appl. Mater. Interfaces*, 2019, **11**, 43608-43621.

3 J. Zhu, Y. Wu, X. Huang, L. Huang, M. Cao, G. Song, X. Guo, X. Sui, R. Ren and J. Chen, *Nano Energy*, 2019, **62**, 883-889.

4 R. Chen, X. Xue, Y. Hu, W. Kong, H. Lin, T. Chen and Z. Jin, *Nanoscale*, 2019, **11**, 13282-13288.

5 J. Zheng, Y. Luo, D. Xie, X. Xiong, Z. Lin, G. Wang, C. Yang and M. Liu, *J. Alloys Compd.*, 2019, **779**, 67-73.

6 J. Xia, L. Liu, S. Jamil, J. Xie, H. Yan, Y. Yuan, Y. Zhang, S. Nie, J. Pan, X. Wang and G. Cao, *Energy Storage Mater.*, 2019, **17**, 1-11.

7 Y. Chen, D. Ge, J. Zhang, R. Chu, J. Zheng, C. Wu, Y. Zeng, Y. Zhang and H. Guo, *Nanoscale*, 2018, **10**, 17378-17387.

8 H.-J. Shin, T. H. Kim, S. Abbas, J. Cho and H. Y. Ha, *Chem. Eng. J.*, 2021, **412**, 128614.

9 T. Zhang, L. Zhang, L. Zhao, X. Huang, W. Li, T. Li, T. Shen, S. Sun and Y. Hou, *Small*, 2020, **16**, 202005302.

10 J. Fu, W. Kang, X. Guo, H. Wen, T. Zeng, R. Yuan and C. Zhang, *J. Energy Chem.*, 2020, **47**, 172-179.

11 R. Wang, X. Dai, Z. Qian, S. Zhong, S. Chen, S. Fan, H. Zhang and F. Wu, *ACS Appl. Mater. Interfaces*, 2020, **12**, 31628-31636.

12 S. Fu, J. Chen, X. Wang, Q. He, S. Tong and M. Wu, *Small*, 2020, **16**, 2000040.

13 D. H. Yang, L. Kong, M. Zhong, J. Zhu and X. H. Bu, *Small*, 2019, **15**, e1804058.

14 S. Liang, X. Pei, W. Jiang, Z. Xu, W. Wang, K. Teng, C. Wang, H. Fu and X. Zhang, *Electrochim. Acta*, 2019, **322**, 134696.

15 X. Li, B. Zhou, W. Wang, Z. Xu, N. Li, L. Kuang, C. Li, W. Mai, H. Fu and H. Lv, *J. Alloys Compd.*, 2017, **706**, 103-109.